PHYSICAL REVIEW B VOLUME 58, NUMBER 16 15 OCTOBER 1998-II

Ultrafast electron dynamics in gold nanoshells

R. D. Averitt, S. L. Westcott, and N. J. Halas
Department of Electrical and Computer Engineering and the Center for Nanoscale Science and Technology, Rice University, Houston, Texas 77005

(Received 24 June 1998)

We present ultrafast optical studies on nanoshells, which consist of a nanoscale Au_2S dielectric core surrounded by an ultrathin Au shell. The plasmon frequency of these nanoparticles can be controlled by varying the ratio of the core diameter to shell thickness. By tuning this plasmon peak, we have observed both transient bleaching and transient absorption for Au nanoshells embedded in polyvinyl alcohol. We relate the induced change in transmission of gold nanoshell films to the electron dynamics in the thin gold shell. Our results indicate that even when the plasmon frequency is shifted below the onset of interband transitions, interband effects are still of primary importance in determining the nonlinear optical response. An electron relaxation time of 1.65 ± 0.10 ps is measured that corresponds to an electron-phonon coupling constant of 2.2×10^{16} W/(m^3 K), smaller than that observed in bulk Au films. [S0163-1829(98)50740-0]

Metal and semiconducting nanoparticles show great promise for application in future optical and electronic devices.[1–4] In particular, the optical properties associated with the plasmon resonance of solid metal nanoparticles have been actively studied for many years.[5] Nonetheless, important advances are still being made regarding the fundamental optical properties of solid metal nanoparticles.[6]

A number of significant experiments have been performed on solid metal nanoparticles with fs time resolution.[7–11] These studies elucidate the relaxation mechanisms of excited electrons in confined metal nanostructures. A study of the differential change in transmission of a solid gold nanoparticle film demonstrated that the plasmon resonance is damped due to increased electron-electron scattering upon heating the conduction electrons.[8] Femtosecond studies of copper and silver nanoparticles showed evidence for a nonthermal electron distribution, similar to what has been observed for thin metal films.[7,12] These studies also measured a longer electron-phonon relaxation time when probing at the plasmon resonance as compared to probing off resonance. This phenomenon has been attributed to resonant plasmon emission by excited electron-hole pairs in the nanoparticle.[13] There have also been studies indicating that size and surface dependent effects can modify the electron dynamics of solid metal nanoparticles.[9,11]

Our recent efforts have focused on the optical properties of a new nanoparticle we call metal nanoshells, which consist of a dielectric core surrounded by a thin metallic shell of nanometer dimensions.[14,15] The optical properties of these nanoparticles are dominated by the response of the metallic shell layer, strongly similar to solid metal nanoparticles. A unique feature of metal nanoshells, in contrast to solid metal nanoparticles, is that the plasmon frequency is a function of the core-shell ratio of the nanoparticle.[14] For a given core radius, a thinner shell will have its plasmon resonance shifted to longer wavelengths in comparison to a particle with a thicker shell. For Au-coated Au_2S nanoshells, the plasmon resonance can be placed from ~ 600 nm to greater than 1100 nm, extending over the tuning range of a Ti:sapphire laser. This has allowed us to study the electron dynamics of a series of gold nanoshell films with the plasmon resonance shifted both above and below the laser wavelength.

Utilizing fs pump-probe spectroscopy, we have observed both transient bleaching and transient absorption in Au/Au_2S nanoshells of ~ 40 nm diameter embedded in polyvinyl alcohol (PVA). Our calculations, which take into account the dipole polarizability (which dominates in this size regime) of the composite gold nanoshells, indicate that the induced change in transmission of nanoshell films is due to the modification of the electron dynamics within the thin gold shell. Additionally, from the measured decay time of 1.65 ps, a value of 2.2×10^{16} W/(m^3 K) is obtained for the electron-phonon coupling constant. Our experimental results are also consistent with the creation of a nonthermal electron distribution that decays to a hot Fermi distribution during the initial ~ 100 fs after excitation.

These experiments utilized a cavity-dumped Ti:sapphire laser operating at 800 kHz producing nominally 50 fs pulses.[16] A cavity-dumped laser allows for greater pulse energy extraction from the laser than standard output coupling. In addition, the lower repetition rate eliminates excessive heating of the sample. A standard pump-probe geometry was used to measure the pump induced change in the nanoshell film transmission. Prism-pair dispersion compensation was used to keep the pulse width below 60 fs at the experiment. Typical pulse fluences ranged from 100 to 400 μJ/cm^2.

A series of gold nanoshells was prepared via reduction of gold chloride with sodium sulfide. The reaction was allowed to proceed to completion with the final location of the plasmon absorption peak determined by reactant concentrations. A JEOL JEM-2010 transmission electron microscope (TEM) was used to image the nanoshells and determine their size distribution.[17] Comparison of the UV-visible extinction spectra with theory allowed us to estimate the average shell thickness for each sample.[14] To make the nanoshell films, approximately 20 μl of a nanoshell concentrate, obtained via centrifugation, was diluted in about 1 ml of a 20% PVA solution. A few drops of the resulting solution were then placed on a microscope slide and allowed to dry. The only change in the nanoshell films as compared to the correspond-

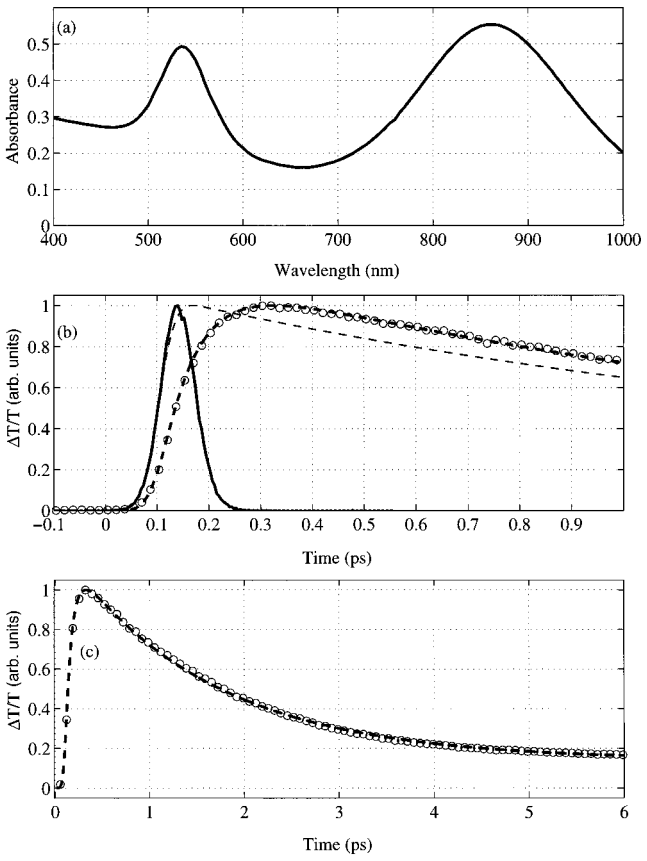

FIG. 1. (a) UV-vis of gold nanoshell film. TEM analysis of this sample gives $r=20.7$ nm and calculations give $r-r_c=3.3$ nm where r_c is the core radius. (b) Open circles: Experimental transient bleaching at 805 nm. Solid line: Autocorrelation at the sample point corresponding to 60 fs Gaussian pulses. Thick dashed line: Fit of data using Eq. (1) convolved with a 60 fs pulse. Thin dashed line: Exponential decay convolved with 60 fs Gaussian pulse. (c) Expanded view of (b).

ing aqueous solution nanoshells was a slight shift ($\sim$50 nm) of the plasmon peak to longer wavelengths due to the change in the dielectric constant of the embedding medium. The films were nominally 50 μm thick with a nanoshell volume filling factor of $\sim 1\times 10^{-5}$.

Figure 1(a) shows the UV-visible spectrum (UV-vis) of a gold nanoshell PVA film that has a plasmon resonance maximum at 865 nm. The peak at $\sim$520 nm is due to the presence of solid gold nanoparticles that form during the growth of the gold-coated gold sulfide nanoparticles.[14,18] The open circles in Fig. 1(b) show the pump-induced change in film transmission ($\Delta T/T$) with the laser tuned to 805 nm. The solid line is the laser autocorrelation at the sample point. This clearly shows a delay in the peak of the photoinduced bleaching signal with respect to the peak in the autocorrelation. This delay has been observed on metal films and Cu nanoparticles and is consistent with the creation of a nascent nonequilibrium electron population that thermalizes to a hot Fermi distribution on a 100 fs time scale.[7,19] The thick dashed line is a fit using the following expression convolved with a 60 fs Gaussian pulse:

$$\Delta T/T=\left[1-\exp\left(\frac{-t}{\tau_r}\right)\right]\exp\left(\frac{-t}{\tau_d}\right)+\Upsilon_{off}. \qquad (1)$$

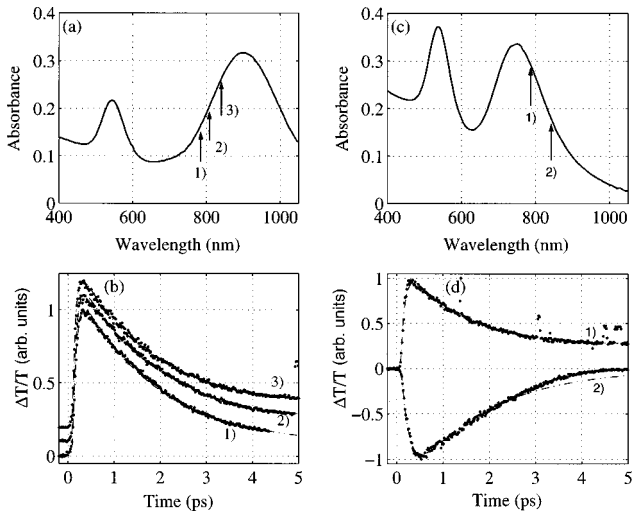

FIG. 2. (a) and (c) show the UV-vis of films corresponding to $\Delta T/T$ data in (b) and (d), respectively. From TEM analysis and calculations: (a) $r=20.9$ nm and $r-r_c=2.8$ nm. (d) $r=21.6$ nm and $r-r_c=3.1$ nm.

This equation results from an extension of the two temperature model (TTM) to include an expression related to the energy stored in the nonthermal electron distribution.[20] A best fit of the data gives a thermalization time $\tau_r=70$ fs and $\tau_d=1.55$ ps. The 1.55 ps decay corresponds to a return of the hot Fermi electron distribution to equilibrium with the lattice of the nanoparticle and the embedding medium. The offset $\Upsilon_{off}=0.15$ is due to temperature dependent effects that persist on a time scale longer than the experiment. The thin dashed line is an exponential decay of 1.55 ps convolved with a 60 fs Gaussian pulse: this functional form cannot be made to fit the data for any value of the lifetime. Figure 1(c) shows the same experimental data and the fit out to 6 ps. This shows that the fit using Eq. (1) is excellent out to longer times.

Figures 2(a) and 2(c) show the UV-vis of two gold nanoshell films with their peak plasmon absorptions at 905 nm and 750 nm, respectively. The numbered arrows in Figs. 2(a) and 2(c) denote the center wavelength of the Ti:sapphire laser, and the corresponding transient change in transmission of the gold nanoshell films is displayed in Figs. 2(b) and 2(d). The gold nanoshell film in Fig. 2(a) has its plasmon peak at a lower energy with respect to the laser for all three scans shown in Fig. 2(b). Figure 2(b) shows that in tuning across the high-frequency edge of the plasmon peak a transient bleaching signal with a lifetime of 1.65 ± 0.10 ps is measured. Several other gold nanoshell films (not shown) having plasmon peaks below the laser energy also displayed induced bleaching with a $\sim$1.65 ps lifetime. For the data in Fig. 2(d), in which the laser is tuned across the low-frequency edge of the plasmon peak, a crossover from transient bleaching to transient absorption is observed. In this regime, the measured lifetimes ranged from 1.2 to 1.8 ps because the broad laser spectrum (full width at half maximum 30 nm) overlaps the crossover from bleaching to absorption. Since bleaching and absorption contribute to the measured signal, it is difficult to extract an unambiguous lifetime over this range. In short, Fig. 2 shows that, in addi-

tion to having tunable linear optical properties, gold nanoshells also have tunable nonlinear optical properties with ps recovery times.

The induced change in transmission ($\Delta T/T$) for gold nanoshell films on an ultrafast time scale is due to the modification of the metallic shell dielectric function upon pump-induced heating of the conduction electrons within the shell. The maximum $\Delta T/T$, which occurs approximately 100 fs after pump excitation, can be calculated using the following equation:

$$\frac{\Delta T}{T} = -\frac{3nl\rho}{2\epsilon_0 \lambda r^3}\left(\frac{\partial \alpha''}{\partial \epsilon_s'}\Delta\epsilon_s' + \frac{\partial \alpha''}{\partial \epsilon_s''}\Delta\epsilon_s''\right). \qquad (2)$$

In this equation, $\epsilon_s = \epsilon_s' + i\epsilon_s''$ is the wavelength dependent dielectric function of the gold shell and α'' is the imaginary part of the gold nanoshell dipole polarizability $\alpha = \alpha' + i\alpha''$. An analytical expression for the polarizability of a nanoshell can be derived by solving Laplace's equation for a shell geometry.[21] The wavelength in vacuum is specified by λ, n is the index of refraction of the embedding medium, l is the film thickness, ρ is the nanoparticle filling fraction, r is the total radius of the gold nanoshell, and ϵ_0 is the free space permittivity. Equation (2) assumes a low nanoshell filling fraction and that $\Delta T/T$ is dominated by induced changes in the real and imaginary parts of the gold shell dielectric function. These are denoted as $\Delta\epsilon_s'$ and $\Delta\epsilon_s''$, respectively. This is reasonable given that the plasmon resonance arises from absorption by the conduction electrons in the thin gold shell. Furthermore, we apply Eq. (2) to calculate the maximum $\Delta T/T$. Temporally, this maximum occurs before any significant change in the dielectric function of the nanoshell core or embedding medium due to heat diffusion could take place.

In order to estimate the magnitude and sign of $\Delta T/T$ using Eq. (2), $\Delta\epsilon_s'$ and $\Delta\epsilon_s''$ must be calculated at a specific electron temperature. Each of these terms has contributions from the Drude free-electron and interband portions of the dielectric function. To estimate the change in the Drude dielectric function, we rely on Fermi-liquid theory that states that the electron-electron scattering rate τ_{ee}^{-1} is proportional to $(E-E_F)^2$ where E is the electron energy and E_F is the Fermi energy. An estimate for the increase in the total electron scattering rate τ^{-1} is obtained by averaging τ_{ee}^{-1} over the allowed energy range for electron scattering.[8,16]

The change in the imaginary portion of the interband dielectric function due to Fermi smearing is determined by calculating the change in the joint density of states (JDOS) between the d band and conduction band.[20,22] Since the plasmon resonance of gold nanoshells lies below the onset of interband transitions, it might be expected that Fermi-level smearing should be of little consequence in calculating $\Delta T/T$. However, via Kramers-Kronig, there can be a substantial change in the real part of the interband dielectric function due to Fermi-level smearing that extends well below the onset of interband transitions. Physically, this corresponds to modified screening by the hot conduction electrons of the d-band electrons associated with the gold ionic cores.

The results of the calculations of $\Delta T/T$ versus wavelength using Eq. (2) are shown in Figs. 3(a) and 3(b). An electron temperature of $T_e = 800$ K is used based on estimates of the experimental T_e from the absorbed pulse fluence and nanoshell concentration. The solid line is the calculated $\Delta T/T$, the dashed line is the contribution to $\Delta T/T$ due to changes in ϵ_s', and the dot-dashed line is due to changes in ϵ_s''. The triangles in Figs. 3(a) and 3(b) are experimentally measured values of the peak transient change in $\Delta T/T$ of the films shown in Figs. 1(a) and 2(c), respectively. There is good agreement between the calculations and the experimental values suggesting that the origin of the $\Delta T/T$ signal is due to the induced changes in ϵ_s upon creation of a hot Fermi electron distribution.

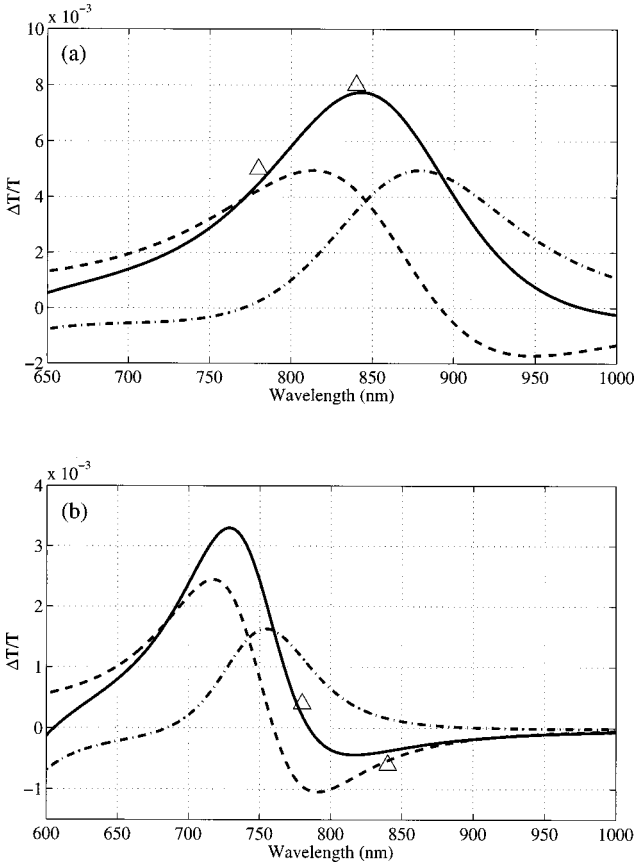

FIG. 3. (a) and (b) show the calculated maximum $\Delta T/T$ for the films in Figs. 1(a) and 2(c), respectively. The electron temperature is $T_e = 800$ K. Solid line: Total $\Delta T/T$. Dashed line: contributions to $\Delta T/T$ from $\Delta\epsilon_s'$. Dashed-dotted line: contributions to $\Delta T/T$ from $\Delta\epsilon_s''$. The triangles are experimental points with a fluence corresponding approximately to $T_e = 800$ K.

Figure 3(b) shows that the calculations predict the crossover from transient bleaching to transient absorption. The dashed line in Fig. 3 shows that the transient absorption arises from changes in ϵ_s'. If the interband contribution to ϵ_s' is not included in the calculations, the predicted magnitude of the induced absorption is a factor of 10 smaller than that experimently observed. This indicates that less efficient screening by the hot conduction electrons is responsible for the observed transient absorption at wavelengths greater than 780 nm.

As the hot Fermi electron distribution returns to equilibrium, $\Delta T/T$ decreases. From the observed 1.65 ps decay of $\Delta T/T$ an electron-phonon coupling constant for gold nanoshells in PVA can be determined using the TTM.[23–25]

The results of this analysis yield an electron-phonon coupling constant $G = 2.2 \times 10^{16}$ W/(m^3 K). For bulk gold films, $G = 3.5 \pm 0.5 \times 10^{16}$ W/(m^3 K) which, in the perturbative limit, corresponds to a lifetime of ~ 800 fs.[25] The relaxation in bulk is faster than for nanoshells due to a greater phonon density of states and more efficient coupling of the electrons to the bulk gold lattice.[26] In contrast, for solid gold nanoparticles with diameters ranging from 14 to 40 nm, lifetimes of 3.5 ps and 7 ps were measured in cyclohexane and water, respectively.[27] The relaxation in the nanoshells is faster, most probably due to the thin shell (< 5 nm) and the large surface area in comparison to the solid gold nanoparticles. The dephasing of the plasmon resonance of nanoshells is dominated by electron surface scattering and therefore it might be expected that electron surface scattering is also an important energy relaxation channel for the electrons.[14] Although the precise microscopic mechanism is not yet understood, studies on solid gold and solid gallium nanoparticles have shown that the surface does play a role in cooling the hot electrons.[9,27]

In conclusion, we have presented a study of the ultrafast electron dynamics of gold nanoshells. Our results indicate that the creation of a hot electron distribution in the gold shells is responsible for the observed transient changes in the film transmission. The ultrafast electron dynamics in gold nanoshells are due to increased electron-electron scattering and an induced modification in the conduction electron screening of the d-band polarizability. Our current studies aim to elucidate the role of the surface in mediating the relaxation of the hot electrons.

We would like to thank Peter Nordlander for discussions regarding the electron dynamics and D. S. Alavi for providing technical comments about cavity-dumped lasers. We would additionally like to thank the Robert A. Welch Foundation, the National Science Foundation, and the Office of Naval Research for support.

[1] C. P. Collier, R. J. Saykally, J. J. Shiang, S. E. Henrichs, and J. R. Heath, Science **277**, 1978 (1997).

[2] L. Landin, M. S. Miller, M. E. Pistol, C. E. Pryor, and L. Samuelson, Science **280**, 262 (1998).

[3] D. C. Ralph, C. T. Black, and M. Tinkham, Phys. Rev. Lett. **78**, 4087 (1997).

[4] V. L. Colvin, M. C. Schlamp, and A. P. Alivisatos, Nature (London) **370**, 354 (1994).

[5] U. Kreibig and M. Vollmer, *Optical Properties of Metal Clusters* (Springer, New York, 1995).

[6] T. Klar, M. Perner, S. Grosse, G. von Plessen, and J. Feldmann, Phys. Rev. Lett. **80**, 4249 (1998).

[7] J.-Y. Bigot, J. C. Merle, O. Cregut, and A. Daunois, Phys. Rev. Lett. **75**, 4702 (1995).

[8] M. Perner, P. Bost, U. Lemmer, G. von Plessen, J. Feldmann, U. Becker, M. Mennig, M. Schmitt, and H. Schmidt, Phys. Rev. Lett. **78**, 2192 (1997).

[9] M. Nisoli, S. Stagira, S. D. Silvestri, A. Stella, P. Tognini, P. Cheyssac, and R. Kofman, Phys. Rev. Lett. **78**, 3575 (1997).

[10] J. H. Klein-Wiele, P. Simon, and H. G. Rubahn, Phys. Rev. Lett. **80**, 45 (1998).

[11] B. A. Smith, J. Z. Zhang, U. Giebel, and G. Schmid, Chem. Phys. Lett. **270**, 139 (1997).

[12] J.-Y. Bigot, Bull. Am. Phys. Soc. **43**, 194 (1998).

[13] I. E. Perakis, Bull. Am. Phys. Soc. **43**, 601 (1998).

[14] R. D. Averitt, D. Sarkar, and N. J. Halas, Phys. Rev. Lett. **78**, 4217 (1997).

[15] S. J. Oldenburg, R. D. Averitt, S. L. Westcott, and N. J. Halas, Chem. Phys. Lett. **288**, 243 (1998).

[16] R. D. Averitt, Ph.D. thesis, Rice University, 1998.

[17] The size distribution was determined using IMAGE TOOL FOR WINDOWS, version 1.28, from the University of Texas Health Sciences Center at San Antonio, San Antonio, TX, 1996.

[18] H. S. Zhou, I. Honma, H. Komiyama, and J. W. Haus, Phys. Rev. B **50**, 12 052 (1994).

[19] W. S. Fann, R. Storz, H. W. K. Tom, and J. Bokor, Phys. Rev. Lett. **68**, 2834 (1992).

[20] C. K. Sun, F. Vallee, L. H. Acioli, E. P. Ippen, and J. G. Fujimoto, Phys. Rev. B **50**, 15 337 (1994).

[21] A. E. Neeves and M. H. Birnboim, J. Opt. Soc. Am. B **6**, 787 (1989).

[22] R. Rosei, F. Antonnangeli, and U. M. Grassano, Surf. Sci. **37**, 689 (1973).

[23] S. I. Anisimov, B. L. Kapeliovich, and T. L. Perelman, Zh. Eksp. Teor. Fiz. **66**, 776 (1974)].

[24] G. L. Eesley, Phys. Rev. Lett. **51**, 2140 (1983).

[25] R. H. M. Groeneveld, R. Sprik, and A. Lagendijk, Phys. Rev. B **51**, 11 433 (1995).

[26] E. D. Belotskii, S. N. Luk'yanets, and P. M. Tomchuk, Zh. Eksp. Teor. Fiz. **101**, 163 (1992) [Sov. Phys. JETP **74**, 88 (1992)].

[27] J. Z. Zhang, B. A. Smith, A. E. Faulhaber, J. K. Anderson, and T. J. Rosales, *Ultrafast Processes in Spectroscopy* (Plenum, New York, 1996), Vol. IX, pp. 561–565.